Обзор ArXiv: astro-ph, за 10-12 мая 2017 года

От Сильченко О.К.

Astro-ph: 1705.03479

ALMA PIN-POINTS A STRONG OVER-DENSITY OF U/LIRGS IN THE MASSIVE CLUSTER XCS J2215 AT $Z = 1.46$

STUART M. STACH,[1] A. M. SWINBANK,[1] IAN SMAIL,[1] MATT HILTON,[2] J. M. SIMPSON[3]

Draft version May 11, 2017

ABSTRACT

We have surveyed the core regions of the $z = 1.46$ cluster XCS J2215.9−1738 with the Atacama Large Millimeter Array (ALMA). We obtained high spatial resolution observations with ALMA of the 1.2 mm dust continuum and molecular gas emission in the central regions of the cluster. These observations detect 14 significant millimetre sources in a region with a projected diameter of just ~ 500 kpc ($\sim 1'$). For six of these galaxies we also obtain ^{12}CO(2–1) and ^{12}CO(5–4) line detections confirming them as cluster members and a further two millimetre galaxies have archival spectroscopic redshifts which also place them in the cluster. An additional ~ 4 millimetre galaxies have photometric redshifts consistent with cluster membership, suggesting that the bulk ($\geq 12/14$, $\sim 85\%$) of the submillimetre sources in the field are in fact luminous infrared galaxies lying within this young cluster. We then use our sensitive new observations to constrain the dust-obscured star formation activity and cold molecular gas within this well-studied example of a $z \sim 1.5$ cluster. We find evidence that the cooler dust and gas components of these galaxies may have been influenced by their environment reducing the gas reservoir for their subsequent star formation. We conclude that these actively star-forming galaxies have the dynamical masses and stellar population ages expected for the progenitors of massive, early-type galaxies in local clusters.

Keywords: Galaxies: clusters: individual: (XMMXCS J2215.9−1738) – galaxies: evolution – galaxies: formation

Зарегистрированные на 1.25 мм (континуум) источники

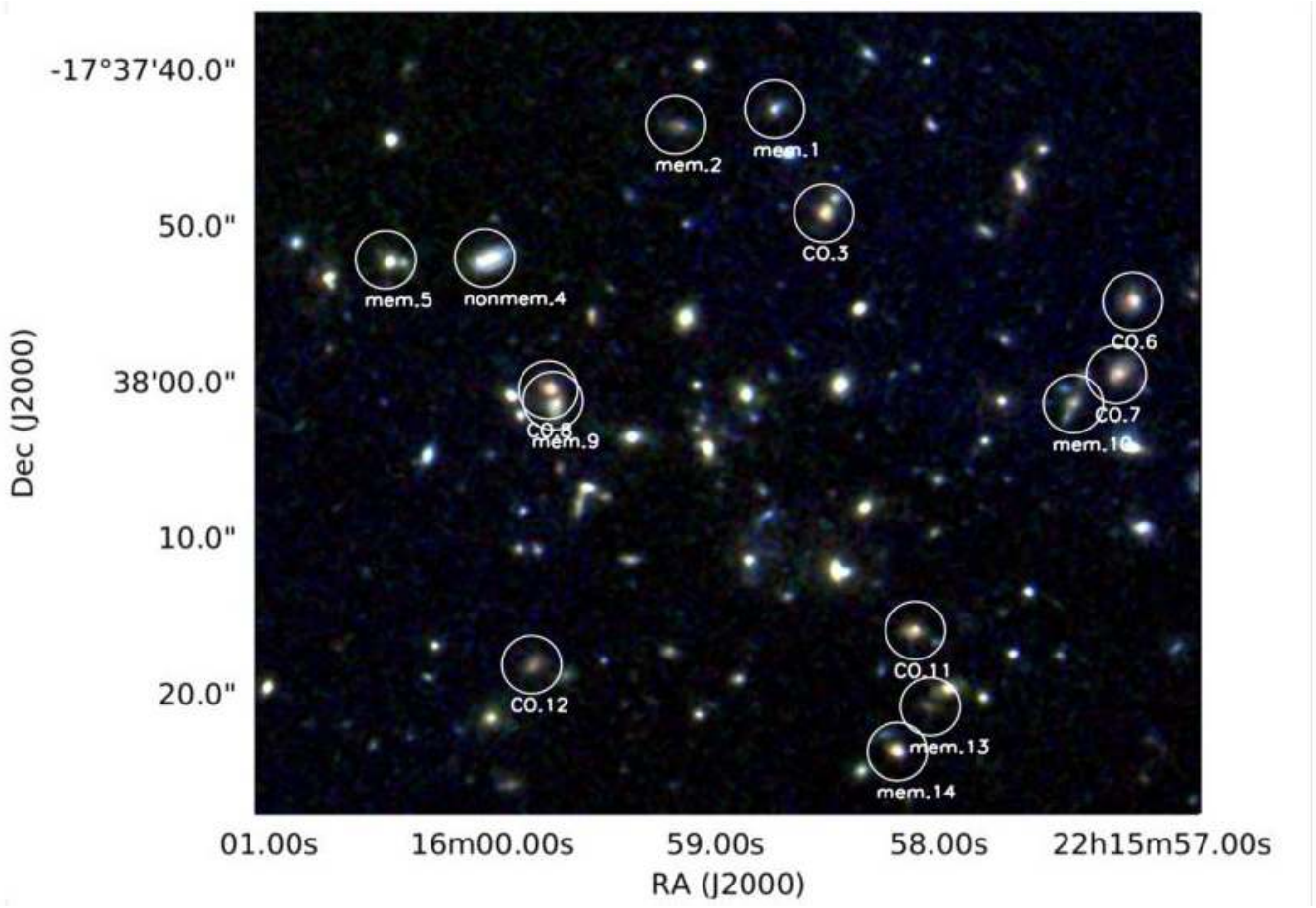

То же самое, по-крупнее

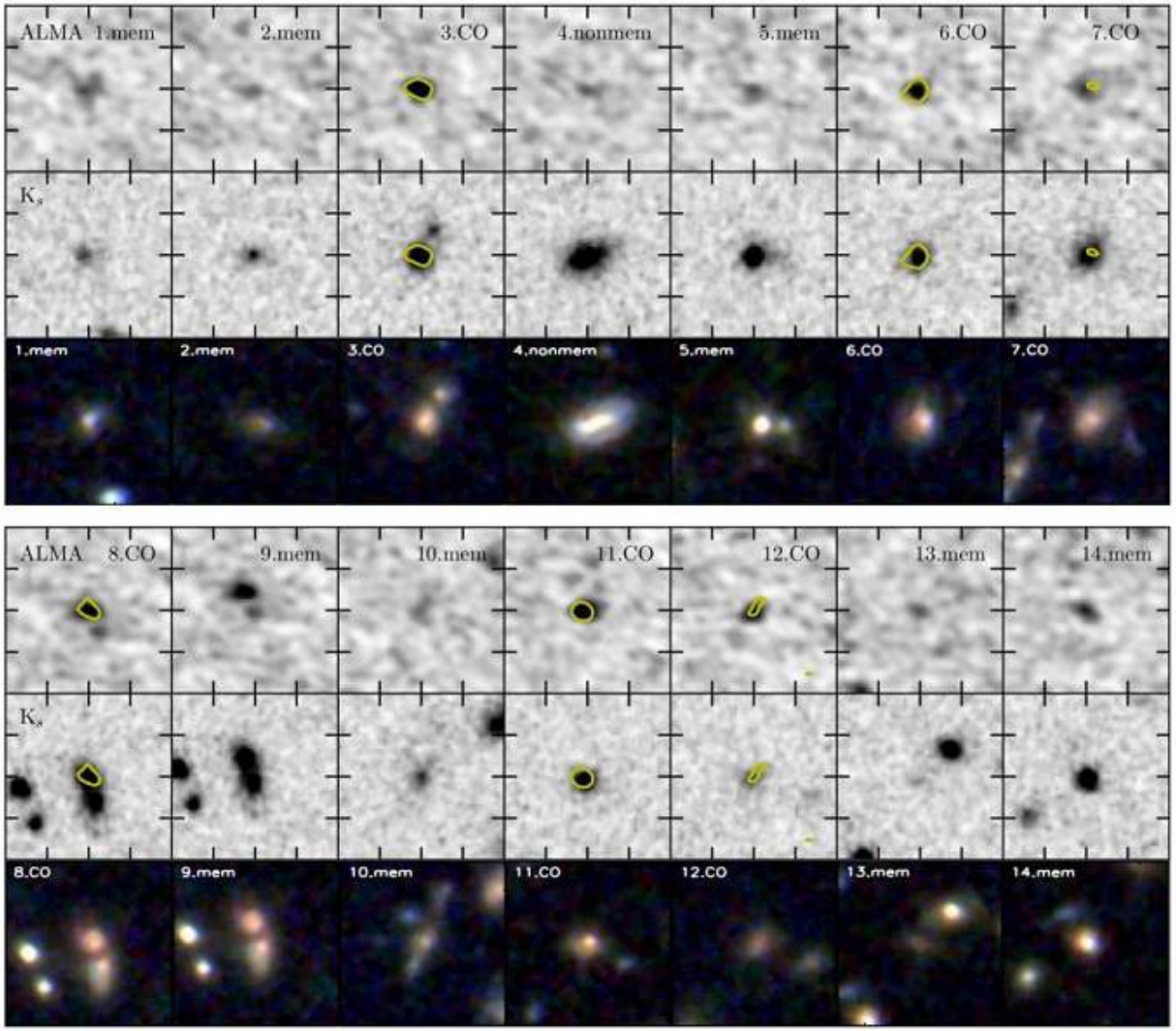

Figure 2. Thumbnails showing the ALMA Band 6 continuum (top row of each panel), K_s (middle row of each panel) and three-colour *HST* WFC3 images (1.25, 1.40 and 1.60 μm, lower row of each panel) of the SNR >4 millimetre continuum sources detected in our map.

Параметры галактик

Table 1
Properties of the ALMA 1.25 mm continuum detections in XCS J2215

ID	R.A. (J2000)	Dec.	$S_{1.25mm}$ (mJy)	L_{FIR} ($10^{11}\,L_\odot$)	SFR ($M_\odot\,yr^{-1}$)	z_p (H09)	z_s^*
1	22 15 58.75	−17 37 40.9	0.46±0.09	$3.5^{+1.9}_{-2.2}$	50^{+30}_{-30}	$1.44^{+1.10}_{-1.10}$	1.460
2	22 15 59.17	−17 37 41.9	0.49±0.08	$2.8^{+1.3}_{-1.4}$	40^{+20}_{-20}	$1.15^{+2.80}_{-0.20}$	...
3	22 15 58.54	−17 37 47.6	0.93±0.05	$8.8^{+4.4}_{-2.2}$	130^{+60}_{-30}	$1.99^{+0.39}_{-0.57}$	**1.453**
4	22 15 59.98	−17 37 50.5	0.21±0.04	$3.6^{+2.1}_{-1.2}$	50^{+30}_{-20}	$1.25^{+0.11}_{-0.36}$	*1.301*
5	22 16 00.40	−17 37 50.6	0.37±0.07	$1.7^{+0.6}_{-0.8}$	20^{+10}_{-10}	$1.33^{+0.69}_{-0.19}$	1.451
6	22 15 57.23	−17 37 53.3	0.68±0.08	$9.4^{+2.7}_{-1.7}$	140^{+40}_{-30}	$1.30^{+0.92}_{-0.48}$	**1.454**
7	22 15 57.30	−17 37 58.0	0.46±0.09	$3.6^{+1.9}_{-2.0}$	50^{+30}_{-30}	$1.35^{+1.00}_{-0.18}$	**1.450**
8	22 15 59.71	−17 37 59.0	0.88±0.08	$3.3^{+0.9}_{-1.1}$	50^{+10}_{-20}	$1.32^{+1.10}_{-0.35}$	**1.466**
9	22 15 59.69	−17 37 59.7	0.28±0.05	$6.7^{+2.5}_{-1.7}$	100^{+40}_{-20}	$1.50^{+0.81}_{-0.22}$	...
10	22 15 57.48	−17 37 59.9	0.18±0.04	$1.8^{+0.8}_{-1.3}$	30^{+10}_{-20}	$1.97^{+0.37}_{-0.61}$	...
11	22 15 58.15	−17 38 14.5	0.98±0.06	$5.5^{+1.6}_{-2.8}$	80^{+20}_{-40}	$1.73^{+0.52}_{-0.36}$	**1.467**
12	22 15 59.78	−17 38 16.7	0.60±0.09	$2.4^{+1.4}_{-1.0}$	40^{+20}_{-10}	$1.54^{+0.86}_{-0.47}$	**1.472**
13	22 15 58.09	−17 38 19.4	0.30±0.07	$3.9^{+1.2}_{-0.6}$	60^{+20}_{-10}	$1.34^{+1.70}_{-0.66}$	...
14	22 15 58.23	−17 38 22.3	0.56±0.08	$3.6^{+2.0}_{-1.9}$	50^{+30}_{-30}	$1.46^{+0.99}_{-0.32}$	...

* Spectroscopic redshifts in **bold** are from ^{12}CO emission, confirmed non-members are in *italics*.

Table 2
Emission line properties for ^{12}CO(2–1) and ^{12}CO(5–4) detections in XCS J2215

ID	$L'_{CO(2-1)}$ (10^{10} K km s^{-1} pc^2)	$FWHM_{CO(2-1)}$ (km s^{-1})	$L'_{CO(5-4)}$ (10^{10} K km s^{-1} pc^2)	$FWHM_{CO(5-4)}$ (km s^{-1})	M_{gas} ($10^{10}\,M_\odot$)	M_{dyn} ($10^{10}\,M_\odot$)
3	1.30±0.3	500±90	0.52±0.07	460±40	2.4±0.7	11±4
6	0.56±0.09	120±30	0.37±0.06	220±20	1.0±0.2	0.6±0.3
7	0.8±0.1	450±100	0.24±0.03	470±60	1.3±0.2	9±5
8	1.5±0.3	440±90	0.46±0.07	510±50	2.2±0.6	9±4
11	0.9±0.2	370±90	0.38±0.06	510±50	1.6±0.5	6±3
12	1.0±0.3	330±100	0.33±0.08	600±100	1.5±0.7	5±3

Вроде как пониженные темпы звездообразования для такого количества газа

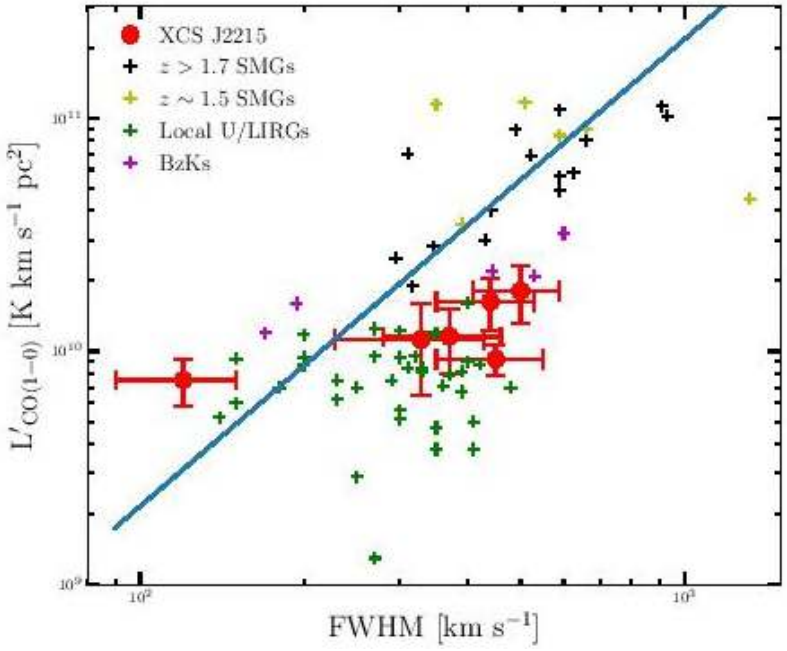

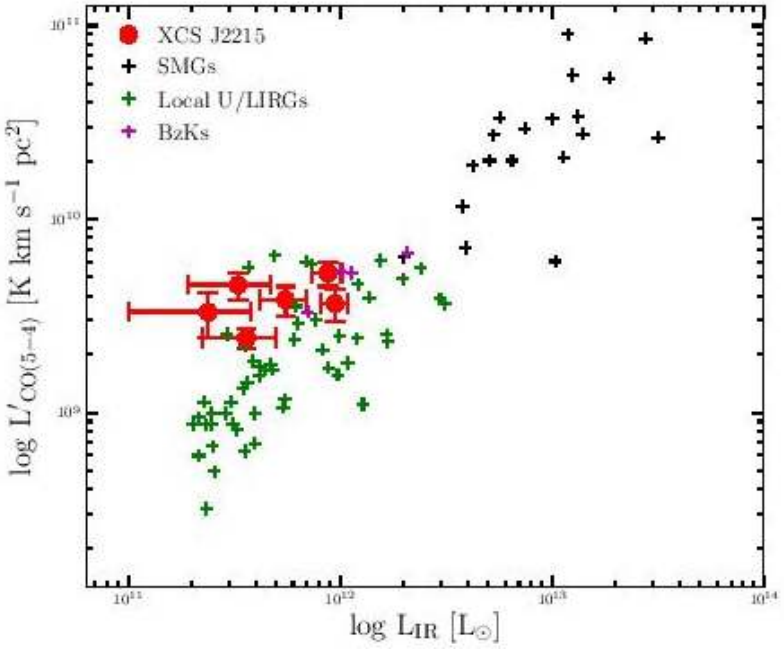

Спекуляции – что будет через 10 млрд лет

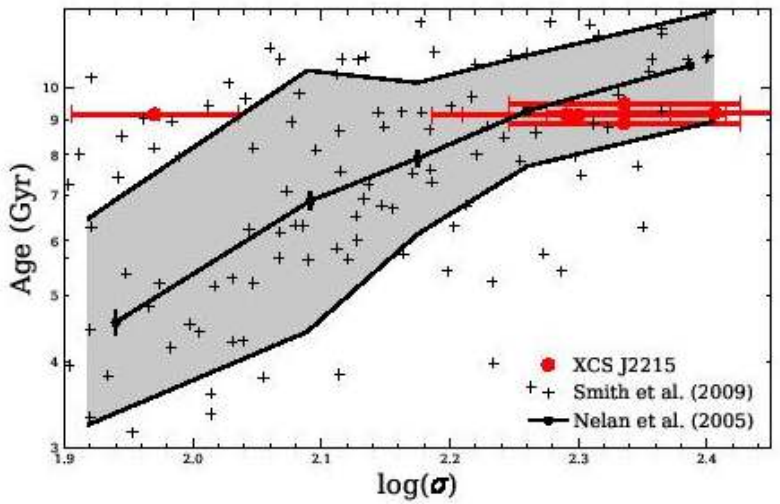

Figure 7. A plot of the velocity dispersion of local early-type galaxies to their luminosity-weighted stellar ages, adapted from (Nelan et al. 2005). We show the median trend line and dispersion derived by (Nelan et al. 2005) and overplot measurements for individual galaxies in the Shapley Supercluster from (Smith et al. 2009) to illustrate the scatter. We plot the velocity dispersions derived from the Gaussian fits to the ^{12}CO lines for the six CO-detected millimetre members in the core of XCS J2215, where their adopted age is the lookback time to $z = 1.46$, 9.3 Gyrs. These points therefore lie where they would appear today if the bulk of their stars

Astro-ph: 1705.03062

ALMA OBSERVATIONS OF GAS-RICH GALAXIES IN $z \sim 1.6$ GALAXY CLUSTERS: EVIDENCE FOR HIGHER GAS FRACTIONS IN HIGH-DENSITY ENVIRONMENTS

A.G. NOBLE,[1] M. MCDONALD,[1] A. MUZZIN,[2] J. NANTAIS,[3] G. RUDNICK,[4] E. VAN KAMPEN,[5] T.M.A. WEBB,[6] G. WILSON,[7] H.K.C. YEE,[8] K. BOONE,[9] M.C. COOPER,[10] A. DEGROOT,[7] A. DELAHAYE,[6] R. DEMARCO,[11] R. FOLTZ,[7] B. HAYDEN,[9,12] C. LIDMAN,[13] A. MANILLA-ROBLES,[5] AND S. PERLMUTTER[9,12]

[1]*Kavli Institute for Astrophysics and Space Research, Massachusetts Institute of Technology, 77 Massachusetts Avenue, Cambridge, MA 02139, USA*
[2]*Department of Physics and Astronomy, York University, 4700 Keele St., Toronto, Ontario, Canada, MJ3 1P3*
[3]*Departamento de Ciencias Físicas, Universidad Andres Bello, Fernandez Concha 700, Las Condes 7591538, Santiago, Región Metropolitana, Chile*
[4]*The University of Kansas, Department of Physics and Astronomy, 1251 Wescoe Hall Drive, Lawrence, KS, 66045, USA*
[5]*European Southern Observatory, Karl-Schwarzschild-Strasse 2 D-85748 Garching bei München, Germany*
[6]*Department of Physics, McGill University, 3600 rue University, Montréal, Québec H3A 2T8, Canada*
[7]*Department of Physics and Astronomy, University of California, Riverside, CA 92521, USA*
[8]*Department of Astronomy and Astrophysics, University of Toronto, 50 St George Street, Toronto, Ontario M5S 3H4, Canada*
[9]*Department of Physics, University of California Berkeley, 366 LeConte Hall MC 7300, Berkeley, CA 94720-7300, USA*
[10]*Department of Physics and Astronomy, University of California, Irvine, 4129 Frederick Reines Hall, Irvine, CA 92697, USA*
[11]*Departamento de Astronomía, Universidad de Concepción, Casilla 160-C, Concepción, Región del Biobío, Chile*
[12]*Physics Division, Lawrence Berkeley National Laboratory, 1 Cyclotron Road, Berkeley, CA 94720, USA*
[13]*Australian Astronomical Observatory, 105 Delhi Road, North Ryde, NSW 2113, Australia*

Submitted to ApJ Letters

Галактики с CO крупным планом

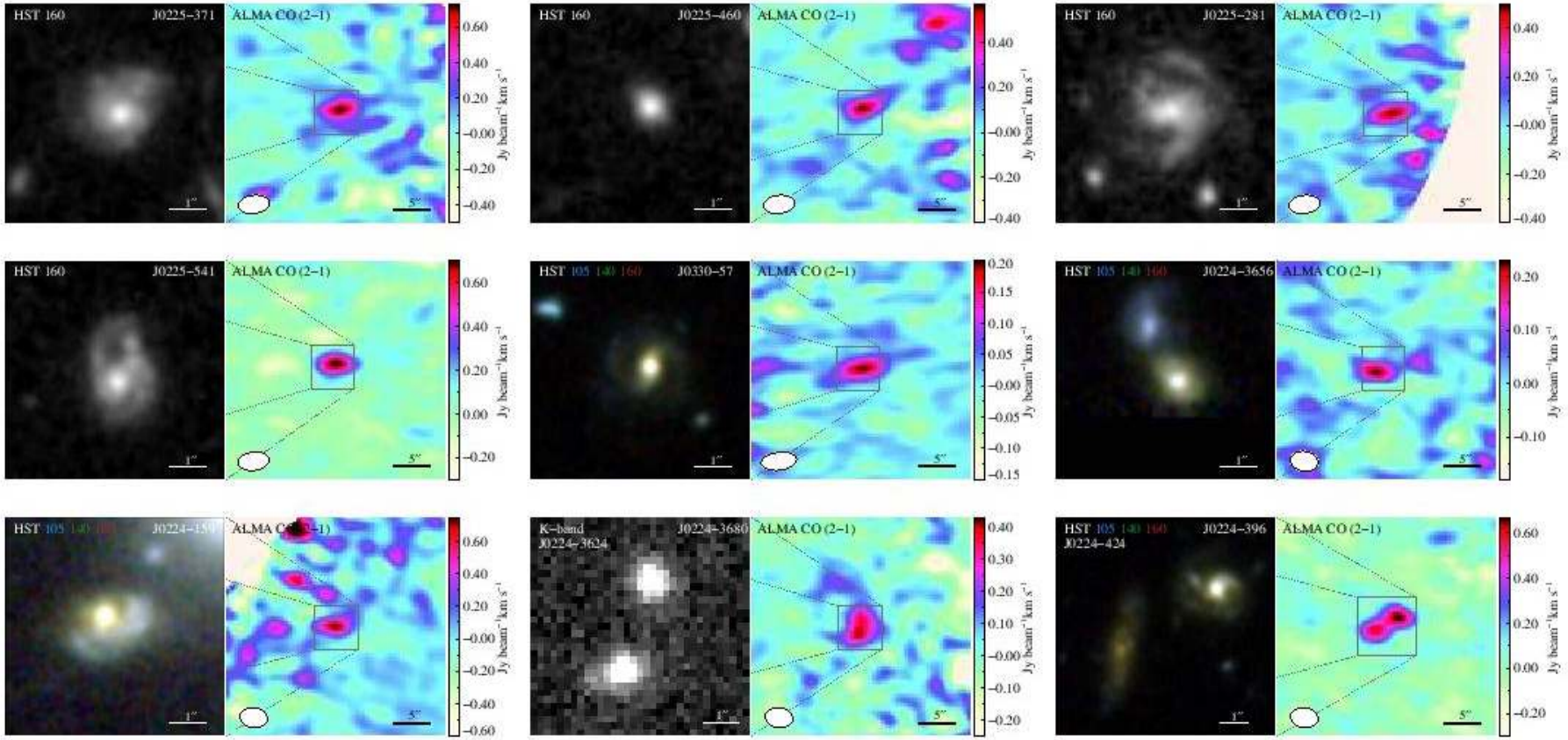

Figure 1. Postage stamps ($30'' \times 30''$) showing the CO (2–1) integrated intensity maps with zoomed-in $6'' \times 6''$ HST images. The synthesized ALMA beam for each map is shown by the white ellipse. We note the blue galaxy to the northeast in J0224-3656 has a photometric redshift of $z = 0.63$ and is thus unlikely to be contributing to the CO flux. The last two stamps in the bottom row represent ALMA pair detections.

Свойства галактик

Table 1. Properties of the CO-detected cluster galaxies

ID	z_{CO}	S/N[a]	$S_{CO}\Delta v$[b] ($Jy\,km\,s^{-1}$)	FWHM[b] ($km\,s^{-1}$)	M_{gas}[c] ($10^{10}\,M_\odot$)	$M_{stellar}$ ($10^{10}\,M_\odot$)	$\langle SFR \rangle$ ($M_\odot\,yr^{-1}$)	f_{gas}	τ (Gyr)
J0225–371	1.599	6.3	1.18±0.18	401±71	21.9±3.4	$6.3^{+0.8}_{-0.9}$	106±19	$0.78^{+0.03}_{-0.04}$	2.1±0.5
J0225–460	1.601	5.8	0.63±0.11	509±104	11.7±2.1	$9.1^{+6.0}_{-3.5}$	86±17	$0.56^{+0.17}_{-0.10}$	1.4±0.4
J0225–281	1.610	6.2	0.59±0.16	122±34	11.1±3.1	$6.5^{+1.7}_{-1.8}$	97±16	$0.63^{+0.09}_{-0.09}$	1.1±0.4
J0225–541	1.611	14.0	0.70±0.06	307±31	13.3±1.2	$6.6^{+0.8}_{-0.9}$	73±17	$0.67^{+0.03}_{-0.03}$	1.8±0.5
J0330–57	1.613	5.2	0.31±0.13	155±40	5.9±2.5	$3.3^{+1.8}_{-1.5}$	38±11	$0.64^{+0.16}_{-0.14}$	1.6±0.8
J0224–3656	1.626	6.8	0.30±0.06	539±113	5.8±1.1	$10.0^{+1.2}_{-4.4}$	42±15	$0.37^{+0.05}_{-0.11}$	1.4±0.6
J0224–159	1.635	5.2	0.46±0.11	245±68	8.9±2.1	$5.9^{+2.6}_{-1.1}$	134±43	$0.60^{+0.12}_{-0.07}$	0.7±0.3
J0224–3680/3624[d,e]	1.626	7.0	1.07±0.19	776±192	20.5±3.6	$9.1^{+3.5}_{-1.5}$	67±15	$0.69^{+0.09}_{-0.05}$	3.1±0.9
J0224–396/424[d]	1.634	9.9	1.32±0.12	493± 53	25.5± 2.4	$16.2^{+3.7}_{-2.4}$	147±21	$0.61^{+0.06}_{-0.04}$	1.7±0.3

[a] Computed from the peak flux and noise in the collapsed image cube.

[b] Computed from a Gaussian fit to the spectral profile.

[c] Calculated using $r_{21} = 0.77$, $\alpha_{CO} = 4.36$.

[d] Pair galaxies, where the CO luminosity and SFR have been measured for the combined pair system.

[e] Spectral profile is fit with a double Gaussian.

Повышенное содержание газа?

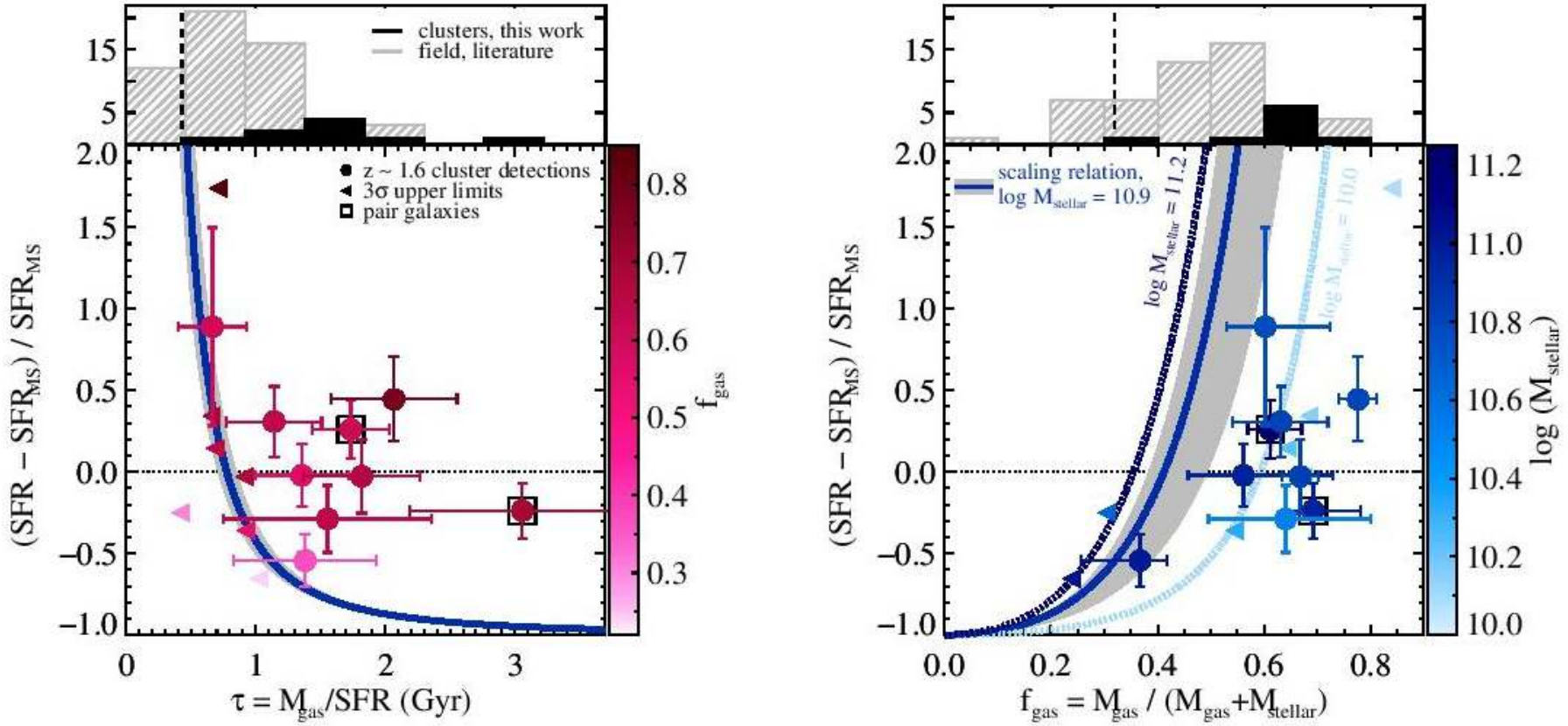

Figure 2. The relative offset from the star-forming main sequence as a function of molecular gas depletion timescale (left) and gas fraction (right). The $z \sim 1.6$ cluster galaxies (circles) are color-coded by the gas fraction (left) and stellar mass (right). Left-facing triangles correspond to 3σ upper limits for spectroscopically-confirmed star-forming cluster members that are not detected in CO (color-coded by their 3σ upper limit in $f_{\rm gas}$ on the left). The solid blue line (grey region) in both panels represents the field scaling relations (1σ fit uncertainties) from Genzel et al. (2015), which have been plotted at $z = 1.6$ and normalized to the average mass of our cluster sample. In the right panel, we also include the scaling relations at the upper and lower mass limits. The upper panels show the binned distribution of each quantity for our cluster galaxies (filled black) and a similar redshift field sample (lined grey) taken from the literature. The vertical black dashed lines represent the

Astro-ph: 1705.03402

Mon. Not. R. Astron. Soc. **000**, 1–15 (xxxx) Printed 10 May 2017 (MN LATEX style file v2.2)

The effect of the environment on the structure, morphology and star-formation history of intermediate-redshift galaxies

Kshitija Kelkar[1⋆],Meghan E. Gray[1], Alfonso Aragón-Salamanca[1],
Gregory Rudnick[2], Bo Milvang-Jensen[3], Pascale Jablonka[4], Tim Schrabback[5]
[1]*School of Physics & Astronomy, University of Nottingham, Nottingham NG7 2RD, UK*
[2]*Department of Physics and Astronomy, University of Kansas, KS 66045-7582*
[3]*Dark Cosmology Centre, Niels Bohr Institute, University of Copenhagen, Juliane Maries Vej 30, 2100, Copenhagen, Denmark*
[4]*Laboratoire d'Astrophysique, cole Polytechnique Fdrale de Lausanne (EPFL), Observatoire de Sauverny, 1290, Versoix, Switzerland; GEPI, Observatoire de Paris, CNRS UMR 8111, Universit Paris Diderot, 92125, Meudon Cedex, France*
[5]*Argelander Institut fuer Astronomie, Auf dem Huegel 71, D-53121 Bonn, Germany*

Выборка – скопления и поле

Table 1. Summary of the cluster sample properties (including secondary clusters identified along the line-of-sight, cf. §2.1), sorted according to cluster halo mass. Columns 1–5 contain the cluster ID, cluster redshift, cluster velocity dispersion, cluster halo mass (calculated following Finn et al. 2005) and the number of spectroscopically confirmed cluster members (Halliday et al. 2004; Milvang-Jensen et al. 2008).

Cluster	$z_{\rm cl}$	$\sigma_{\rm cl}$ (km s^{-1})	log $M_{\rm cl}$ ($M_\odot$)	No. of spec. members
Clusters				
cl1232−1250	0.5414	1080^{+119}_{-89}	15.21	54
cl1216−1201	0.7943	1018^{+73}_{-77}	15.06	67
cl1138−1133	0.4796	732^{+72}_{-76}	14.72	49
cl1354−1230	0.7620	648^{+105}_{-110}	14.48	22
cl1054−1146	0.6972	589^{+78}_{-70}	14.38	49
cl1227−1138	0.6357	574^{+72}_{-75}	14.36	22
cl1138−1133a	0.4548	542^{+63}_{-71}	14.33	14
cl1037−1243a	0.4252	537^{+46}_{-48}	14.33	43
cl1054−1245	0.7498	504^{+113}_{-65}	14.16	36
cl1040−1155	0.7043	418^{+55}_{-46}	13.93	30
cl1227−1138a	0.5826	432^{+225}_{-81}	13.69	11
Groups				
cl1103−1245a	0.6261	336^{+36}_{-40}	13.66	15
cl1037−1243	0.5783	319^{+53}_{-52}	13.61	16
cl1103−1245b	0.7031	252^{+65}_{-85}	13.27	11

Table 2. Details of the full spectroscopic sample and subsample, divided by environment and morphology. The subsample has a stellar mass-completeness of log $M_*/M_\odot = 10.6$.

Spectroscopic sample		E	S0	Sp	Irr	Total
Cluster	All	104	46	195	16	361
	Mass-complete	65	30	95	4	194
Field	All	31	9	91	20	151
	Mass-complete	15	6	35	1	57

Параметры (пекулярной) морфологии

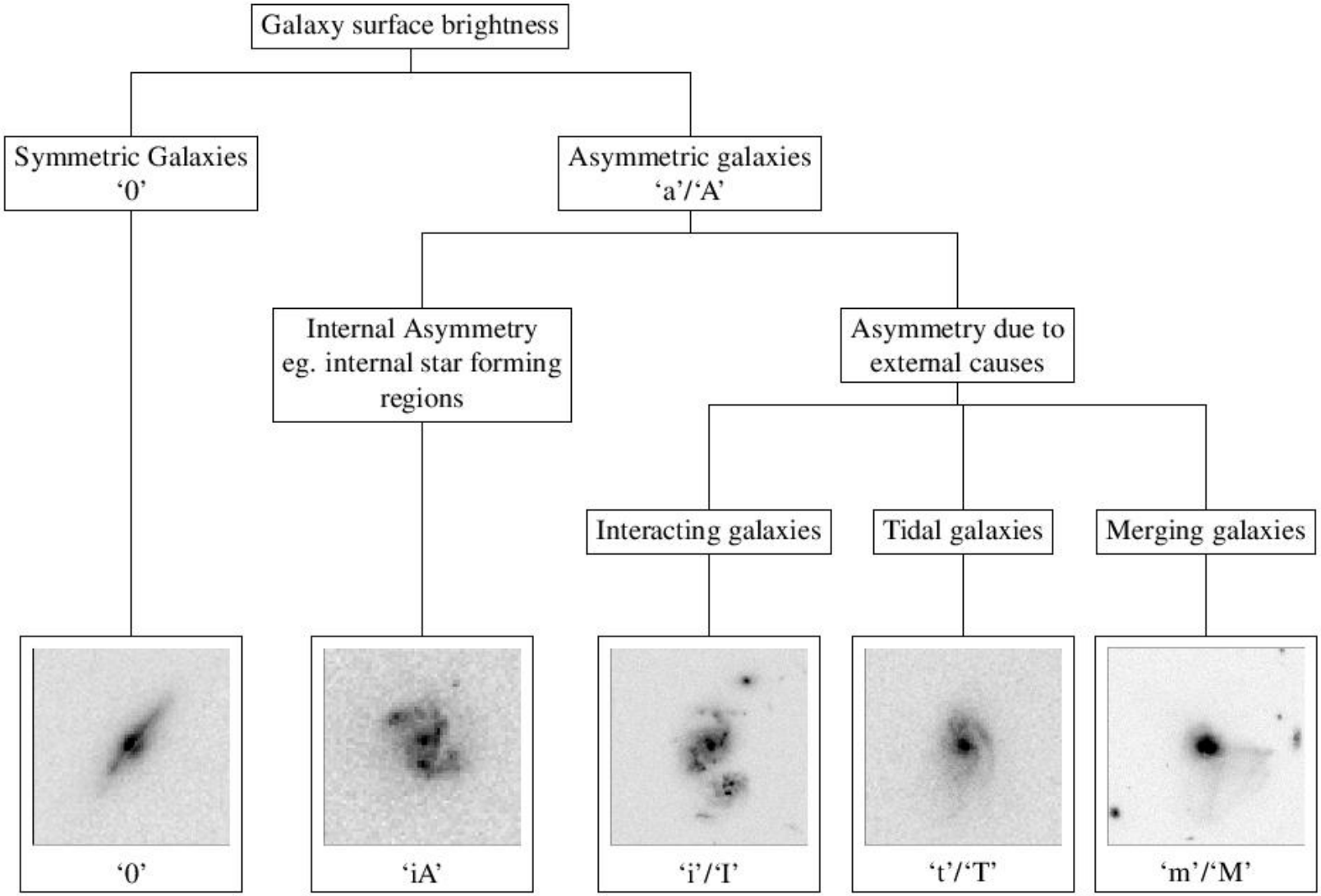

Статистика пекулярной морфологии

Table 3. The relative fractions for galaxies identified as undisturbed, internally asymmetric (possessing asymmetry but with no obvious external cause), interacting galaxies, tidal galaxies and galaxies experiencing an ongoing merger, for a fixed morphology in cluster and field environment. Refer to Section 6 for detailed discussion.

Morphology	**Environment**	Undisturbed (0)	Internally asymmetric (iA)	Interacting (i/I)	Tidal (t/T)	Merger (m/M)
Ellipticals (E)	Cluster	0.79±0.04	0.01±0.01	0.17±0.04	0.02±0.01	0.02±0.01
	Field	0.64±0.08	0.08±0.05	0.14±0.06	0.11±0.05	0.08±0.05
Lenticulars (S0)	Cluster	0.93±0.04	0.01±0.01	0.07±0.04	0.01±0.01	0.01±0.01
	Field	0.85±0.11	0.05±0.05	0.15±0.11	0.05±0.05	0.05±0.05
Spirals (Sp)	Cluster	0.35±0.03	0.25±0.03	0.18±0.03	0.09±0.02	0.11±0.02
	Field	0.36±0.05	0.22±0.04	0.20±0.04	0.11±0.03	0.11±0.03
Irregulars (Irr)	Cluster	0.03±0.03	0.38±0.12	0.15±0.08	0.09±0.06	0.32±0.11
	Field	0.02±0.02	0.21±0.09	0.12±0.07	0.21±0.09	0.40±0.11

Классификация по звездообразованию

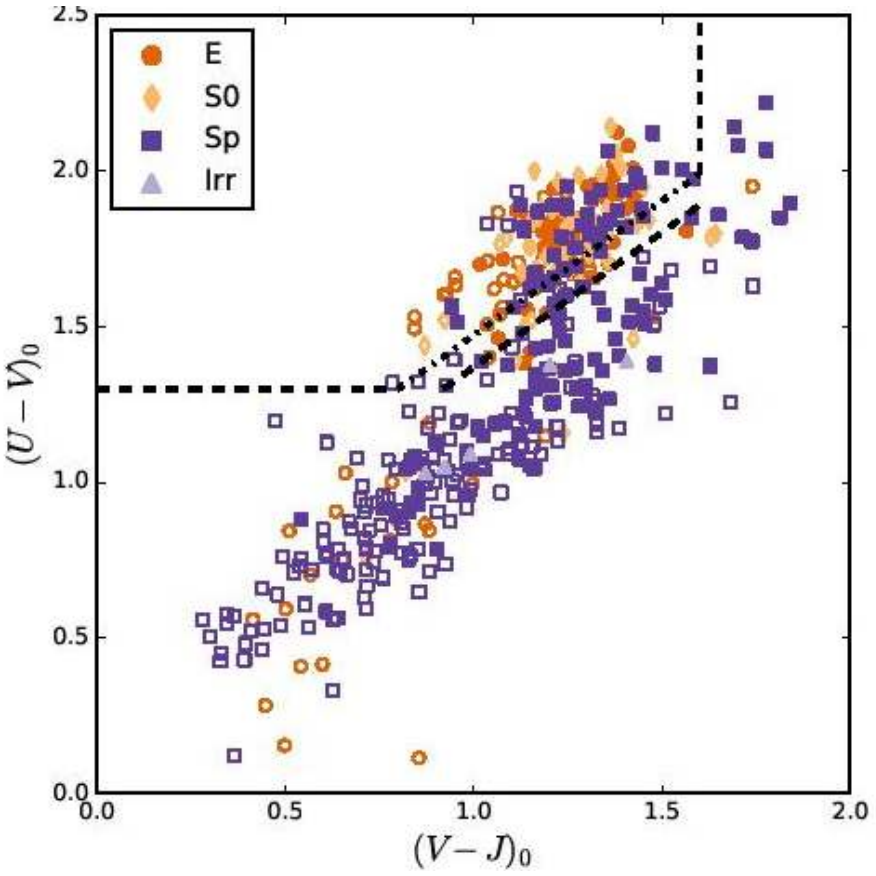

Разнообразные статистики

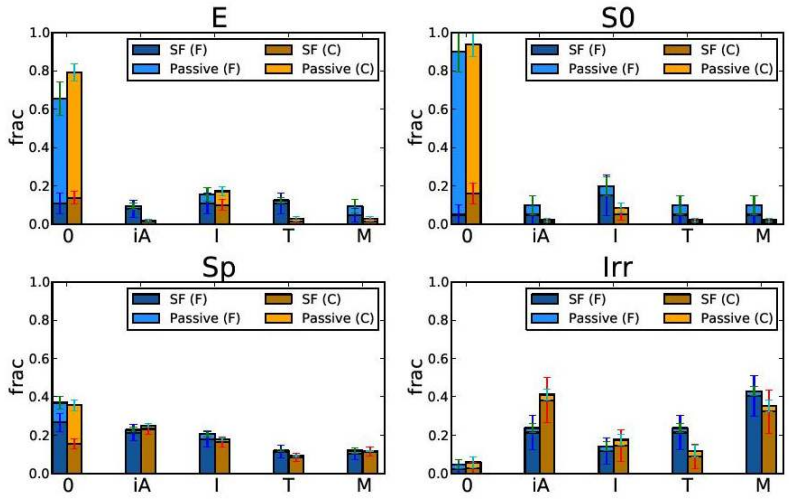

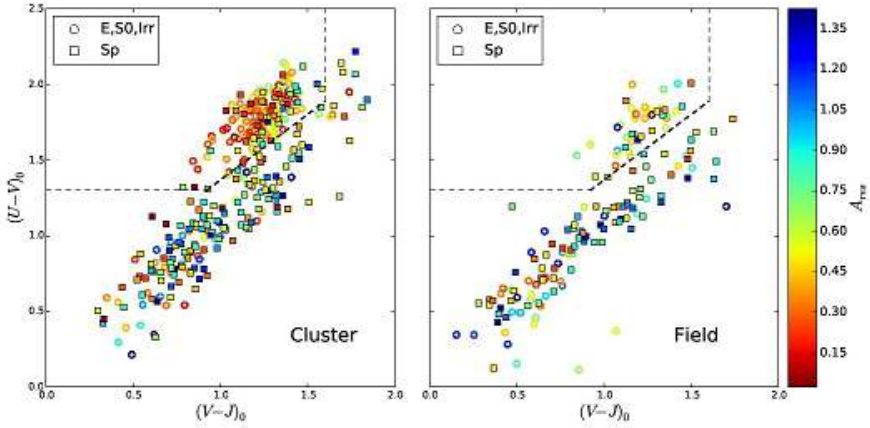

Figure 9. Similar to Figure 8, the UVJ plot is here colour-coded according to A_{res} for cluster (left panel) and field (right panel) galaxies. Star-forming galaxies are consistently found to be more quantitatively asymmetric than passive galaxies irrespective of morphology or global environment. Moreover, complementing Figure 8, the passive spirals in clusters are found to be more symmetric with low A_{res}.

Выводы

- As expected, the vast majority of elliptical and S0 galaxies are smooth and symmetric, while all irregular galaxies are "rough" and asymmetric. Statistically, spiral galaxies tend to have higher values of RFF and $A_{\rm res}$ than early-type galaxies.
- Over 60% of all spiral galaxies are visually classified as showing some degree of asymmetry. Of these, about one third exhibit asymmetry of internal origin (due, e.g., to the presence of large star-forming regions), while the rest show signs of galaxy-galaxy interactions, tidal interactions or mergers in comparable proportions.
- In agreement with the results of Hoyos et al. (2016), we find that RFF correlates strongly with the star-formation activity of the galaxies: star-forming galaxies tend to have much "rougher" structures.
- At fixed morphology, there are no significant differences in the distribution of the disturbance classes of cluster and field galaxies.
- About 40% of all the spiral galaxies are classified as symmetric and undisturbed both in clusters and in the field. However, the fraction of these that are passive (i.e., non-starforming) is twice as large in clusters than in the field: about half of the cluster symmetric spirals are passive, vs. only one quarter in the field (with a significance of 2.3σ). These passive spirals are not only visually symmetric, but also quantitatively smoother (i.e., have smaller RFF values) than star-forming ones.
- While nearly all lenticular galaxies are visually symmetric and undisturbed both in clusters and in the field, *all* the field ones are passive, while nearly $\sim$20% in the clusters are star-forming.

Astro-ph: 1705.03839

The effects of the cluster environment on the galaxy mass-size relation in MACS J1206.2-0847

U. Kuchner[1], B. Ziegler[1], M. Verdugo[1], S. Bamford[2], and B. Häußler[3]

[1] Department of Astrophysics, University of Vienna, Türkenschanzstrasse 17, A-1180 Vienna,
[2] School of Physics & Astronomy, The University of Nottingham, University Park, Nottingham, NG7 2RD, UK,
[3] European Southern Observatory, Alonso de Córdova 3107, Casilla 19001, Santiago, Chile
e-mail: ulrike.kuchner@univie.ac.at

ABSTRACT

The dense environment of galaxy clusters strongly influences the nature of galaxies. Their abundance and diversity is imprinted on the stellar-mass–size plane. Here, we study the cause of the size distribution of a sample of 560 spectroscopic members spanning a wide dynamical range down to $10^{8.5}M_{\odot}$ (log(M)-2) in the massive CLASH cluster MACSJ1206.2-0847 at $z = 0.44$. We use Subaru SuprimeCam imaging covering the highest-density core out to the infall regions (3 virial radii) to look for cluster-specific effects on a global scale. We also compare our measurements to a compatible large field study in order to span extreme environmental densities.

Цвет-светимость галактик

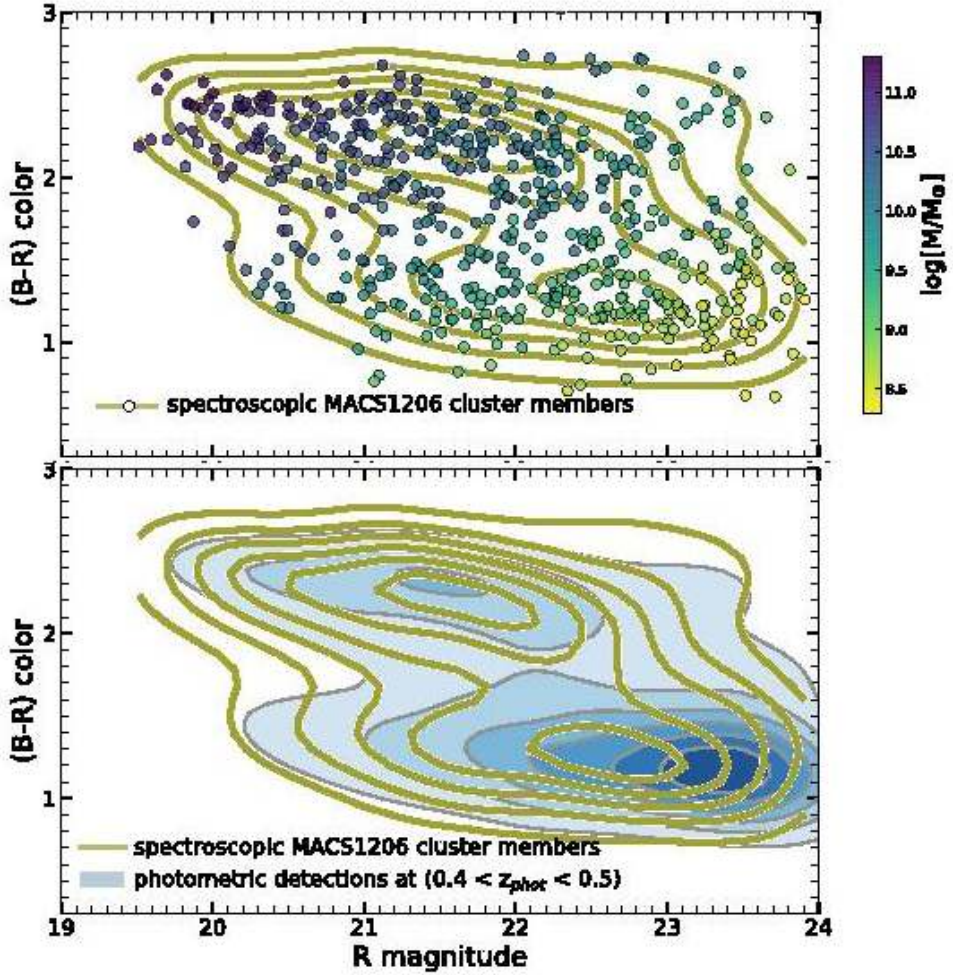

Про скопление

Our sample is comprised of spectroscopic cluster members, the only way to establish cluster membership with high confidence. To distinguish between cluster members and interloping foreground and background galaxies, we assume a cluster mass model assuming a singular isothermal sphere (SIS; Carlberg et al. 1996), thereby identifying cluster membership on the basis of their location in projected phase space. We use the velocity dispersion $\sigma \sim 1087$km/s, virial radius $R_{200} \sim 1.96$, and virial mass $M_{200} \sim 1.37 \times 10^{15} M_{\odot}$ presented in Biviano et al. (2013) for this cluster. For our purpose, we follow the simple approach offered by Carlberg et al. (1997) to identify cluster members as those galaxies with velocities $|v| < 2\sigma(R)$, which is in rough correspondence with the more detailed analysis by Biviano et al. (2013). We also use galaxies between $2\sigma(R) < |v| < 6\sigma(R)$, which are considered galaxies that are falling into the cluster (see

Про звездообразование

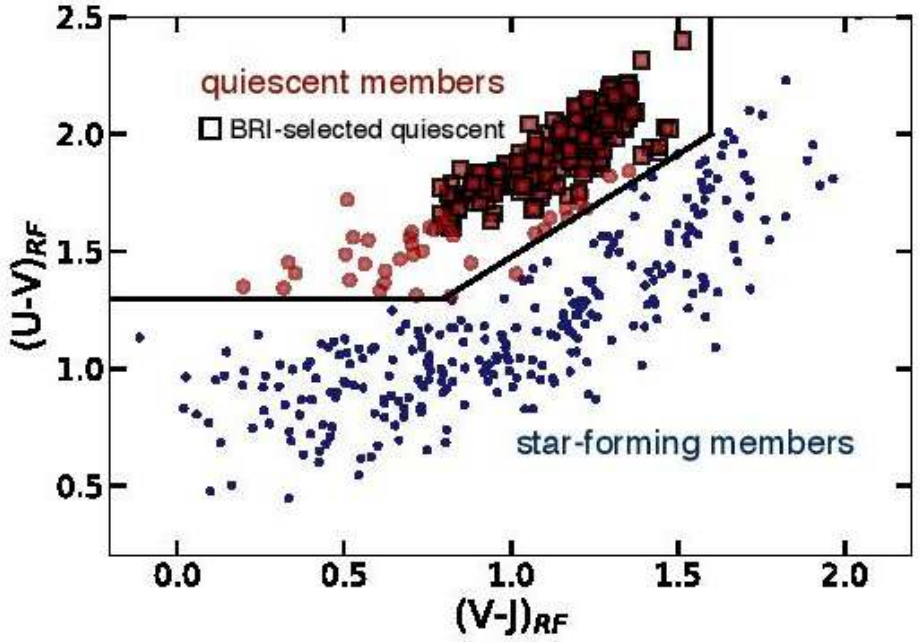

Про морфологию

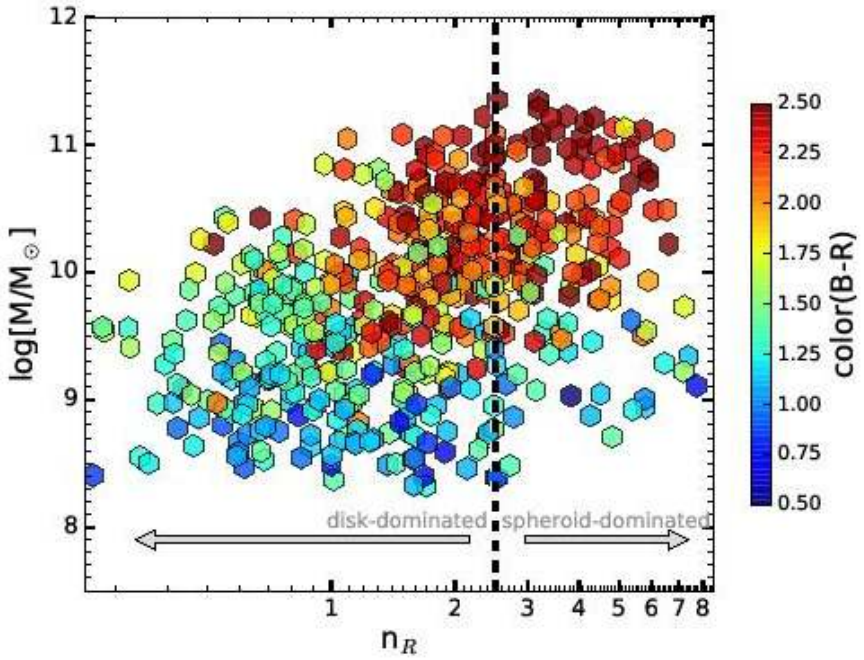

Fig. 3: The 3D distribution of the sample: Sérsic index n versus stellar mass, color coded by their (B-R) colors. The dashed line indicates the hard cut in Sérsic index (n=2.5) used here for the first morphological classification into disk-dominated and spheroid-dominated galaxies.

Про размер!

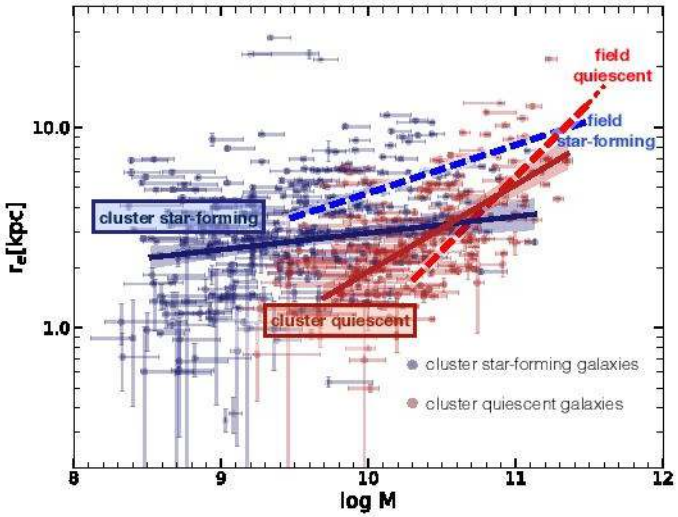

Fig. 4: Comparison of stellar-mass – size relations of cluster galaxies in MACS1206 (solid lines) to field galaxies from (van der Wel et al. 2014) (dashed lines). This simple comparison suggests some minor differences. Points are BRI-selected star-forming (blue) and quiescent (red) cluster galaxies. The blue and red solid lines are single power-law fits to the entire respective weighted data $\log(M/M_\odot) > 8.5$ for star-forming and $\log(M/M_\odot) > 9.2$ for quiescent galaxies (see Appendix A). Er-

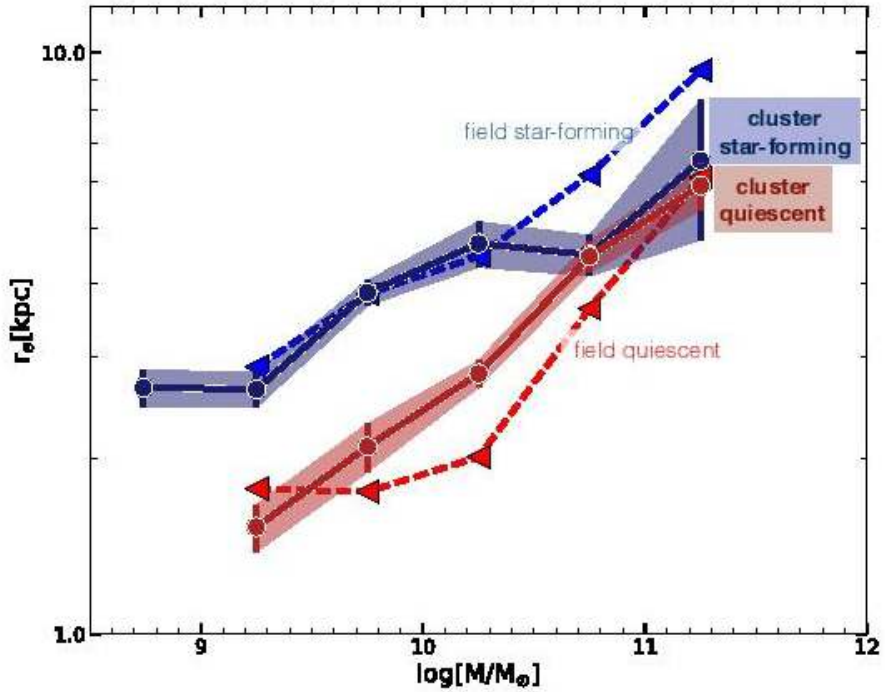

Соотношение размер-масса, с разбивкой по морфологии

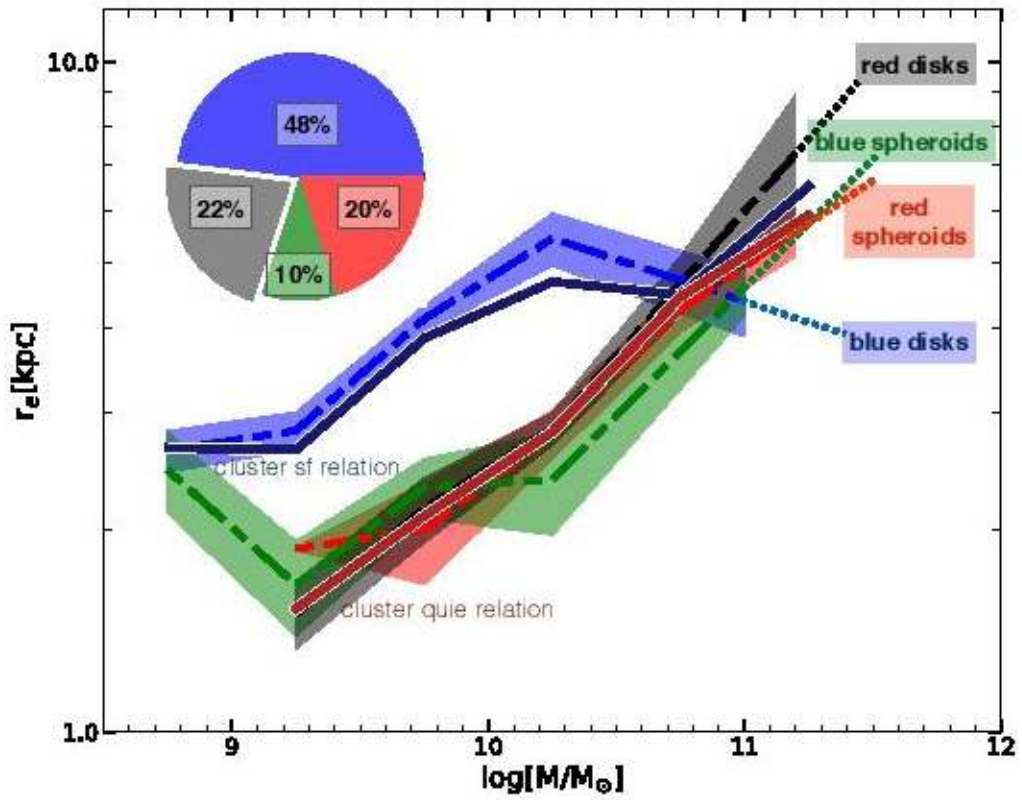

Fig. 7: The stellar-mass – size relation for star-forming galaxies with $n < 2.5$ (blue), star-forming galaxies with $n > 2.5$ (green), and quiescent galaxies with $n > 2.5$ (red), quiescent galaxies with $n < 2.5$ (black). Star-forming disk galaxies are much larger

А это уже только размеры ДИСКОВ

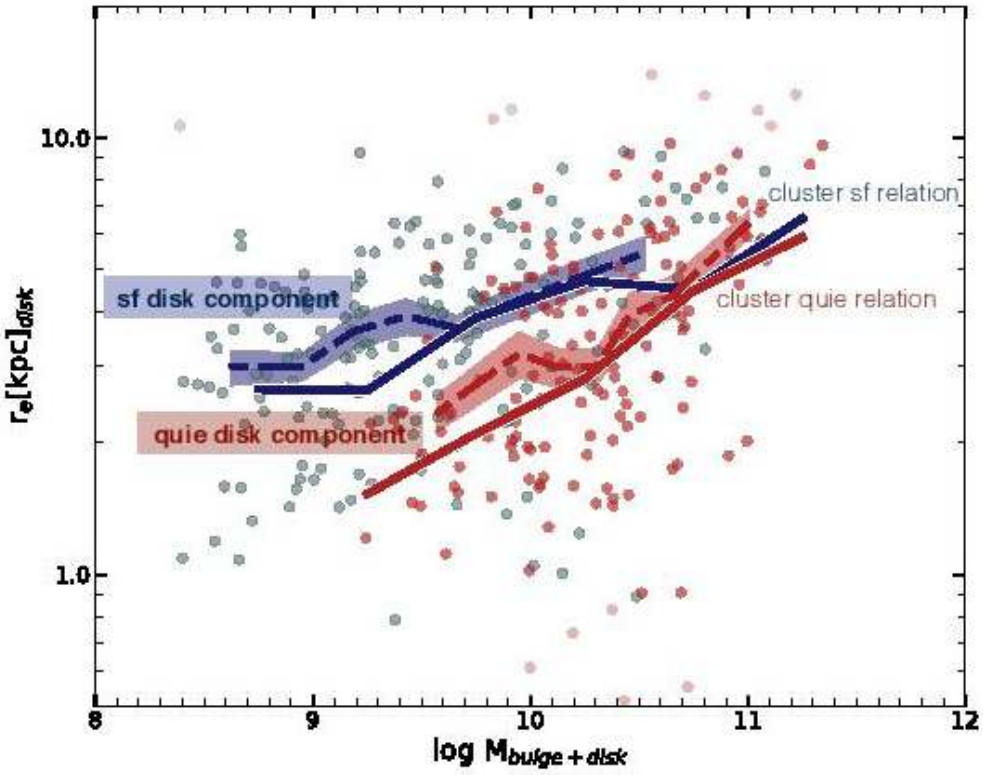

Фазовая диаграмма галактик

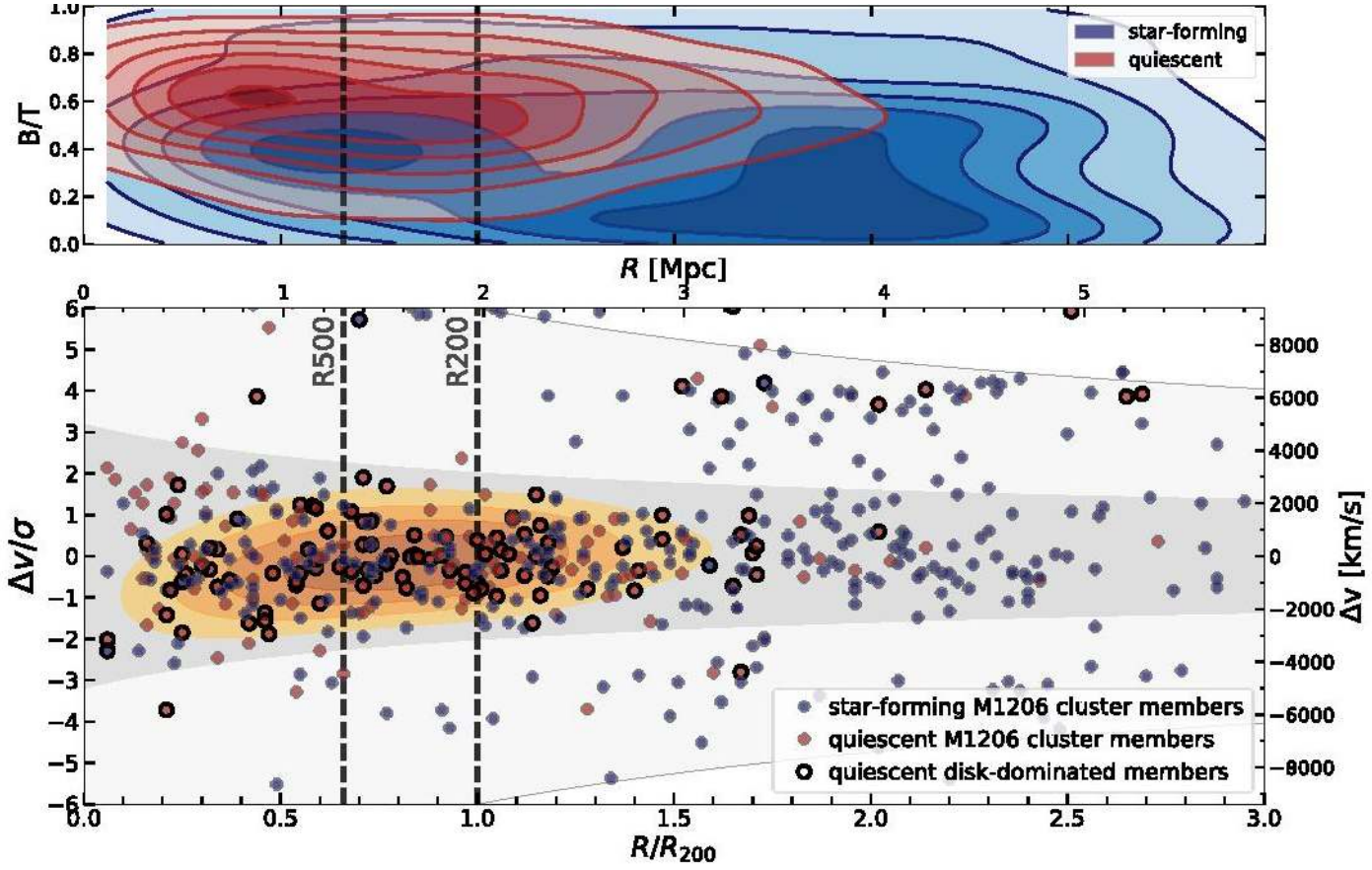

Анализ фазовой диаграммы в цифре

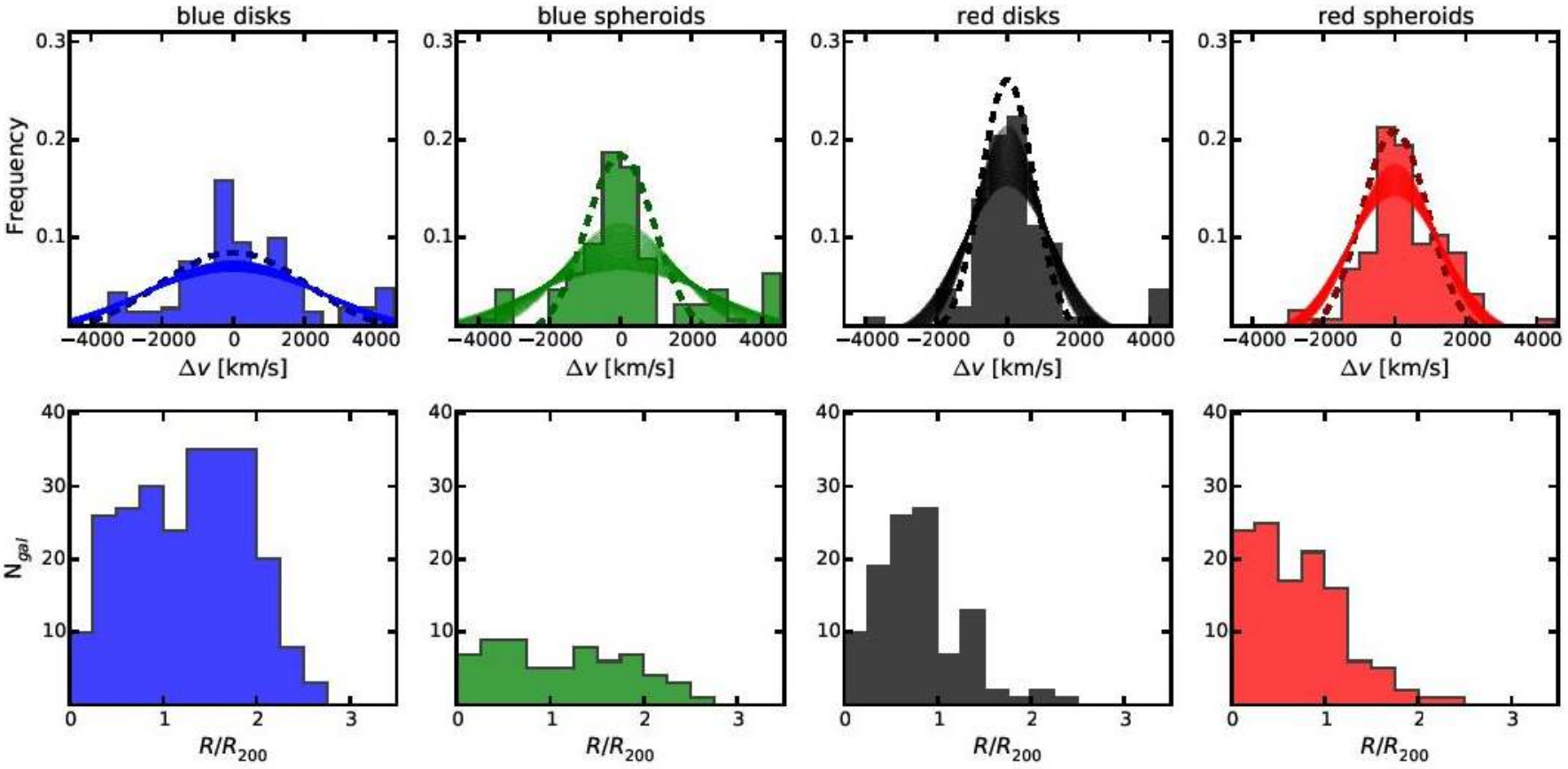

То же самое в таблице.

Table 1: Velocity dispersions for four subgroups of galaxy members and results of their K-S tests

Galaxy sub-population	#	velocity dispersion (2-σ clipped) [km s^{-1}]
blue disks	253	2585 (2117) ±178
blue spheroids	64	2185 (967) ±507
red disks	108	1096 (741)±171(741)
red spheroids	118	1247 (932) ±131

Compared Samples	p-value(%) K-S test
blue disks vs. blue spheroids	6.3
blue spheroids vs. red disks	«1
red disks vs. red spheroids	«1
blue spheroids vs. red spheroids	«1
blue spheroids vs. red disks	«1
red disks vs. red spheroids	2.4

Почему же все-таки красные диски НАСТОЛЬКО меньше голубых?

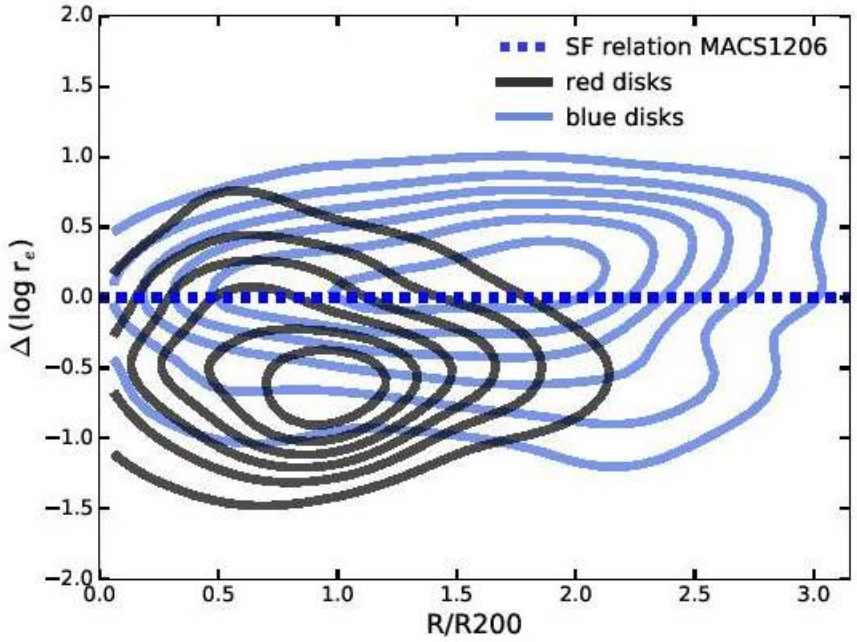

Fig. 14: Differences in size to the star-formation relation (as shown in Fig. 9) vs. cluster-centric distance, normalized by R_{200}. We show density contours for blue and red disk galaxies. At R_{200}, an increasingly important population of "red disk" galaxies is responsible for a decrease of sizes of disk-dominated galaxies.